Geotech Geol Eng (2012) 30:407–417
DOI 10.1007/s10706-011-9476-z

ORIGINAL PAPER

Application of Piezoceramic Elements for Determining Elastic Properties of Soils

A. Patel · K. K. Singh · D. N. Singh

Received: 5 June 2010 / Accepted: 27 October 2011 / Published online: 10 November 2011

Abstract Elastic modulus and Poisson's ratio of soils are two important parameters required for safe design of various civil engineering structures. The elastic modulus and shear modulus of the soils are generally obtained from the resonant column, torsional shear tests and geophysical methods. Though, from these parameters the Poisson's ratio can be determined, these tests are quite elaborate, cumbersome, time consuming and require skilled manpower particularly for data interpretation. Moreover, direct determination of the Poisson's ratio by employing micro-strain gauges, which measure axial and lateral strains using Wheatstone bridge circuits, is difficult for soils due to the problems associated with their fixing on the surface of the sample. Under these circumstances, application of piezoceramic elements, which can generate shear and compression waves, seems to be an excellent alternative. Using these wave velocities, the Poisson's ratio can be computed easily and precisely. However, how this (computed) value of the Poisson's ratio compares vis-à-vis that obtained from the conventional triaxial tests (i.e., strain controlled uniaxial compression tests), which yield stress–strain relationship, needs to be established. With this in view, investigations were conducted on soils of different types (clays and sands) in their disturbed and undisturbed forms by resorting to piezoceramic tests and the triaxial tests. Details of the methodology are presented in this paper and it has been demonstrated that application of piezoceramic elements yields the Poisson's ratio and the elastic modulus of the soils quite easily, particularly for the soft clays and sands.

Keywords Piezoceramic elements · Elastic modulus · Poisson's ratio · Wave velocity · Soils

Abbreviations

A	Maximum amplitude
A_c	Corrected area of the soil sample
C_u	Coefficient of uniformity
d	Piezoelectric charge constant
D_{50}	Effective particle size
D_0	Initial diameter of the soil sample
D_c	Corrected diameter of the soil sample
e	Void ratio

A. Patel
Department of Civil Engineering, VSS University of Technology, Burla, India
e-mail: anjanp14@gmail.com

K. K. Singh
Department of Civil Engineering, IITB-Monash Research Academy, Indian Institute of Technology, Bombay 400076, Mumbai
e-mail: kunal_singh@iitb.ac.in

D. N. Singh (✉)
Department of Civil Engineering, Indian Institute of Technology, Bombay 400076, Mumbai
e-mail: dns@civil.iitb.ac.in

e_{max}	Maximum void ratio
e_{min}	Minimum void ratio
E	Elastic modulus
f	Frequency
G	Shear modulus
G_s	Specific gravity
h	Thickness of the piezoceramic element
Δh	Shear deformation of the piezoceramic element
l	Free length of the piezoceramic element
LL	Liquid limit
M	Constraint modulus
P	Applied load
PI	Plasticity index
PL	Plastic limit
s_u	Undrained shear strength
t	Time-lag between the input and output waves
t_1	Thickness of the central electrode
T	Time period
u_x	Particle motion in x-direction
u_y	Particle motion in y-direction
V	Applied voltage
V_s	Shear wave velocity
V_p	Compression wave velocity
ε_{trans}	Transverse strain
ε_{axial}	Axial strain
κ	Wave number
λ	Wave length
ω	Temporal angular frequency
ρ	Mass density of the soil sample
v	Poisson's ratio
w	Water content
γ_d	Dry density
γ_w	Unit weight of water
γ_t	Bulk density

1 Introduction

Poisson's ratio, v, can be computed by measuring the transverse, ε_{trans}, and axial, ε_{axial}, strains, with the help of strain gauges or LVDTs, by conducting the conventional triaxial tests (i.e., strain controlled uniaxial compression tests) (Bragg and Andersland 1982; Samsuri and Herianto 2004).

$$v = -(\varepsilon_{trans}/\varepsilon_{axial}). \quad (1)$$

However, it must be noted that measurement of ε_{trans} and ε_{axial} for soft clays and sands is quite difficult. On one hand, penetration of LVDTs in soft clays and sands yields inaccurate strains, while on the other hand, fixing micro-strain gauges, which measure axial and lateral strains using Wheatstone bridge circuits, on the surface of these soil samples is a major challenge.

Moreover, Elastic modulus, E, and shear modulus, G, are important parameters required for safe design of various civil engineering structures. Earlier researchers (Kim and Stokoe 1992; Mancuso et al. 2002; Sawangsuriya et al. 2008) have employed resonant column test and the torsional shear test to obtain the E and G, respectively. However, these test methods are cumbersome, time consuming and require skilled manpower. v can be computed by employing Eq. 2 (Luna and Jadi 2000; Santamarina et al. 2001; Zeng and Tammineni 2006), as well.

$$v = (0.5 \times E/G) - 1. \quad (2)$$

Due to these difficulties, researchers (Jain 1988; Lees and Wu 2000; Luna and Jadi 2000; Ayres and Theilen 2001; Landon et al. 2007) have employed geophysical testing methods (viz., seismic refraction and reflection, suspension logging, steady-state vibration, down-hole, seismic cross-hole, spectral analysis of surface waves, SASW, multi-channel analysis of surface waves, MASW, seismic cone penetration tests) for estimating parameters G, and v of the soil mass by employing Eqs 3 and 4, respectively, (Santamarina et al. 2001; Zeng and Tammineni 2006; Phani 2008). It is worth mentioning here that geophysical tests propagate seismic waves through the soil mass at a very low strain level (<0.001%).

$$G = \rho \times V_s^2 \quad (3)$$

$$v = \left(0.5 \cdot \mathrm{r}^2 - 1\right)/\left(\mathrm{r}^2 - 1\right) \quad (4)$$

where, ρ is mass density of the soil mass and, r is the ratio between V_s and V_p, the shear and compression wave velocities, respectively.

However, geophysical methods are quite expensive and require trained and skilled manpower for interpretation of the obtained results. In such a situation, application of piezoceramic elements (i.e., bender and extender elements, which can be used for generating shear and compression waves, respectively) for determining elastic moduli and Poisson's ratio of the soil mass has been found to be quite useful (Agarwal and Ishibashi 1991; Jovicic et al. 1996; Brocanelli and Rinaldi 1998; Lohani et al. 1999; Santamarina et al.

2001; Huang et al. 2004; Bartake et al. 2008). However, how this (computed) value of the Poisson's ratio compares vis-à-vis that obtained from the conventional triaxial tests, which yield stress–strain relationship, needs to be checked.

With this in view, investigations were conducted on soils of different types (clays and sands) in their disturbed and undisturbed forms by resorting to piezoceramic tests and conventional triaxial tests. Details of the methodology to achieve this are presented in this paper and it has been demonstrated that by using piezoceramic elements, the Poisson's ratio and the elastic modulus of the soils can be obtained quite easily, particularly for the soft clays and sands.

2 Experimental Investigations

2.1 Sample Details

In the present study, tests were carried out on three different grades of sands and soft clays. The sands were characterized as SP type as per the USCS (Unified Soil Classification system), the details of which are given in Table 1. The soft clays, characterized as CH type, were collected from the field in their undisturbed form, using Shelby tubes. Soil specimens were then extruded from the sampling tubes using a sample extractor and a hollow cylindrical split mold (38 mm in diameter and 76 mm in length). The water content, w, and bulk density, γ_t, of these specimens vary from 36 to 71% and 14–18 kN/m^3, respectively (refer Table 2). İn order to prepare the sample of the sand, the sand was poured in a plastic cylinder, made of thin polythene sheet (a transperancy sheet, which is less than 1 mm thick), with the help of a glass funnel and by maintaining 30 mm height of the fall. Later, the exact length of the sample was measured on four diametrically opposite sides of the mold and the average of these values was used for determining the initial volume and hence the dry unit weight, γ_d, of the sample. Using these parameters, the initial void ratio, $e[= ((G_s \cdot \gamma_w)/\gamma_d) - 1]$, of the sample was determined. Where, G_s is the specific gravity of the soil and γ_w is the unit weight of water. For achieving different void ratios of the sample, the cylinder containing the sand was subjected to shaking by mounting it on a vibration table for certain duration.

Table 1 Physical characteristics of the sand samples used

Sand	G_s	D_{50} (mm)	C_u	e_{max}	e_{min}
SS1	2.65	1.25	1.97	0.85	0.56
SS2		0.63	1.67	0.86	0.58
SS3		0.33	1.41	0.87	0.58

2.2 Load-Deformation Characteristics

The test setup employed for obtaining the load-deformation characteristics of the soil samples consists of a compression testing machine (supplied by Humboldt, USA), a load cell of 10 kN capacity, and a sample cage made of three derlin rings and the connecting rods (refer Fig. 1). The middle ring can support three LVDTs (Linearly Variable Differential Transducers) at 120° apart, as depicted in Fig. 2. These LVDTs (type KL 17, supplied by KAPTL Instrumentation, India) work on the principle that when AC current (2 Vrms, 5 kHz sine-wave) is applied to primary winding, it produces a magnetic field which, in turn, induces emf-in two differentially connected, secondary windings. The magnetic core moving linearly along the axis varies the flux linkage from primary to both the secondary. The output voltage, thus obtained is linearly proportional to linear displacement. These LVDTs have flat tips, which restricts their piercing into the sample, and can record deformations in the range of 0–10 mm, with a resolution of 1 μm. The undisturbed clay samples were housed inside the cage whereas, in case of sands, a low density polyethylene sheet of thickness 0.1 mm was rolled in the form of a cylinder (height 76 mm and diameter 38 mm), placed inside the cage and was used as a mold for preparing the sample by adopting the rain-fall technique. The LVDTs record ε_{trans} of the sample, when it is axially loaded. For obtaining ε_{axial}, another similar LVDT was employed, which measures the sitting deformation of the soil sample. A 5-channel readout unit, which has a computer interface, was used for recording ε_{trans}, ε_{axial} and the applied load, P. Using these data, the stress-deformation characteristics of the samples were established.

2.3 Shear and Compression Wave velocity Measurement

The piezoceramic elements, used in the present study were developed using a Lead Zirconate Titanate

Table 2 Experimental results obtained for the clay samples

Sample	w (%)	γ_t (kN/m^3)	γ_d (kN/m^3)	$E_{expt.}$ (MPa)	v_{expt}	V_s (m/s)	V_p (m/s)	LL (%)	PL (%)	PI (%)	s_u (kPa)
1	42	14.6	10.3	6.9	0.27	108	203	82	34	48	43
2	47	16.8	11.4	14.4	0.26	115	221	58	27	31	100
3	46	16.5	11.3	7.2	0.35	109	225	63	32	31	117
4	49	16.4	11.0	4.1	0.34	101	155	64	25	39	77
5	47	16.2	11.0	5.4	0.27	121	218	64	25	39	80
6	44	16.2	11.2	7.5	0.25	122	218	62	31	31	99
7	53	15.1	9.9	5.8	0.38	92	173	62	33	29	33
8	45	16.7	11.5	4.9	0.23	98	251	62	31	31	95
9	48	15.3	10.3	7.7	0.24	124	210	64	25	39	88
10	51	17.1	11.4	5.7	0.24	118	210	61	29	32	85
11	55	15.3	9.9	6.8	0.35	90	167	62	33	29	40
12	58	16.1	10.2	6.2	0.31	115	189	82	35	47	52
13	52	17.2	11.3	3.3	0.29	117	189	69	32	37	65
14	60	15.8	9.9	3.0	0.41	77	138	74	30	44	30
15	40	15.6	11.2	10.9	0.26	129	206	63	27	36	150
16	47	16.3	11.1	12.5	0.28	148	234	72	29	43	125
17	51	16.7	11.1	2.5	0.35	113	192	82	34	48	55
18	56	15.5	10.0	2.9	0.39	83	152	59	32	27	30
19	51	15.5	10.8	6.0	0.39	103	201	88	36	52	40
20	62	14.6	9.0	6.3	0.42	96	170	61	34	27	38
21	71	14.3	8.4	0.9	0.21	50	87	62	36	26	14
22	58	16.5	10.5	5.8	0.46	93	173	87	36	51	58
23	57	15.7	10.0	4.7	0.45	109	176	69	32	37	70
24	51	16.9	11.2	7.0	0.37	118	194	66	38	28	92
25	52	15.7	10.3	4.4	0.20	117	186	69	32	37	67
26	55	15.4	10.0	2.2	0.40	98	180	85	36	49	45
27	58	17.0	10.8	2.9	0.33	91	161	78	33	45	50
28	61	15.1	9.4	5.4	0.46	92	144	61	34	27	35
29	46	16.2	11.1	6.6	0.23	145	266	58	27	31	93
30	48	16.1	10.8	6.4	0.23	150	276	64	25	39	87
31	51	17.1	11.3	5.2	0.28	105	195	87	36	51	60
32	57	15.5	9.9	4.3	0.43	97	147	59	32	27	30
33	41	16.4	11.6	14.9	0.30	176	288	63	27	36	142
34	54	15.8	10.3	2.7	0.34	100	173	85	36	49	45
35	49	17.9	12.0	6.3	0.29	113	225	82	34	48	58
36	37	17.1	12.6	10.9	0.17	197	327	78	31	47	212
37	56	16.8	10.8	4.3	0.39	106	170	82	35	47	50
38	54	16.3	10.6	6.4	0.40	118	177	97	37	60	54
39	66	15.3	10.6	2.8	0.46	53	83	59	33	26	26
40	51	17.9	11.8	3.0	0.40	80	138	89	39	50	47
41	64	15.6	9.5	4.2	0.43	108	188	88	36	52	45
42	61	15.9	9.9	3.4	0.45	85	150	82	35	47	52
43	40	17.4	12.4	10.5	0.25	206	318	78	31	47	205
44	48	17.6	11.8	8.0	0.19	125	243	62	31	31	91

Table 2 continued

Sample	w (%)	γ_t (kN/m^3)	γ_d (kN/m^3)	$E_{expt.}$ (MPa)	v_{expt}	V_s (m/s)	V_p (m/s)	LL (%)	PL (%)	PI (%)	s_u (kPa)
45	55	14.8	9.5	2.1	0.31	102	162	82	35	47	45
46	41	17.5	12.4	12.7	0.19	125	243	78	31	47	185
47	51	15.5	10.3	5.1	0.27	103	167	97	37	60	63
48	53	14.9	9.8	6.2	0.42	124	231	87	36	51	65
49	47	15.7	10.7	3.7	0.22	90	164	48	25	23	100
50	52	14.6	9.6	6.0	0.29	90	189	64	25	39	74
51	54	16.7	10.8	6.3	0.42	97	158	97	37	60	59
52	56	14.8	9.5	5.1	0.42	105	176	78	33	45	52
53	47	15.9	10.8	11.4	0.28	126	221	61	29	32	118
54	58	15.1	9.6	3.5	0.27	83	146	78	38	40	35
55	47	16.4	11.2	5.7	0.23	84	146	58	27	31	92
56	62	15.6	9.7	2.4	0.46	56	82	58	33	25	16
57	57	14.9	9.5	8.0	0.46	96	183	88	36	52	43
58	61	14.6	9.1	2.8	0.43	77	145	76	30	46	27
59	50	17.0	11.4	5.7	0.35	76	143	64	25	39	84
60	58	15.0	9.5	4.1	0.26	53	81	74	31	43	33
61	51	16.5	10.9	7.1	0.30	97	152	58	27	31	91
62	58	16.1	10.2	8.4	0.42	96	157	67	32	35	48
63	36	17.5	12.9	18.5	0.29	106	327	78	31	47	293
64	40	17.8	12.7	12.0	0.19	200	303	78	31	47	182
65	59	16.6	10.4	6.0	0.43	92	171	67	32	35	45
66	62	13.3	8.2	6.7	0.38	55	86	59	33	26	30
67	53	17.0	11.1	2.3	0.24	71	146	97	37	60	51
68	68	15.0	8.9	2.9	0.46	59	117	58	33	25	15
69	55	16.3	10.5	1.6	0.43	49	81	36	18	18	23
70	67	14.6	8.7	2.6	0.38	56	120	58	33	25	18
71	47	16.0	10.9	3.3	0.31	92	173	69	32	37	62
72	64	16.9	10.3	4.9	0.34	97	152	97	37	60	53
73	54	16.9	10.9	5.6	0.27	112	248	61	29	32	81
74	70	15.4	9.0	2.1	0.46	51	81	67	34	33	24
75	49	14.6	9.8	5.3	0.26	138	273	64	25	39	79

(LZT) based material, SP-5A, corresponding to the US DOD (Department of Defense) Navy type material-II. The reason behind choosing this grade of the piezoceramic material is its high dielectric constant, with high piezoelectric sensitivity, which makes it an ideal material for low power applications. Moreover, this grade of the material exhibits excellent time stability as well and the "time lag" between the voltage application and wave generation is quite low. Different properties of this piezoceramic element are listed in Table 3.

Two sets of piezoceramic elements (15 × 12 × 0.65 mm) as depicted in Fig. 3 were fabricated. One set was polarized in same direction while the other set is polarized in the opposite direction. The centre and the two outer electrodes (made of deposited silver) were soldered to stranded wires. This enables the piezoceramic elements to act as series- or parallel-type, respectively, as depicted in Fig. 4. The solder composition is 62% tin, 36% lead and 2% silver and the soldering time was kept as short as possible to avoid any depoling of the piezoceramic elements. It can be mentioned here that a piezoceramic element can act as a bender or extender depending upon the wiring configuration (series/parallel) and direction of polarization (same/opposite) of the bimorphs (Lings

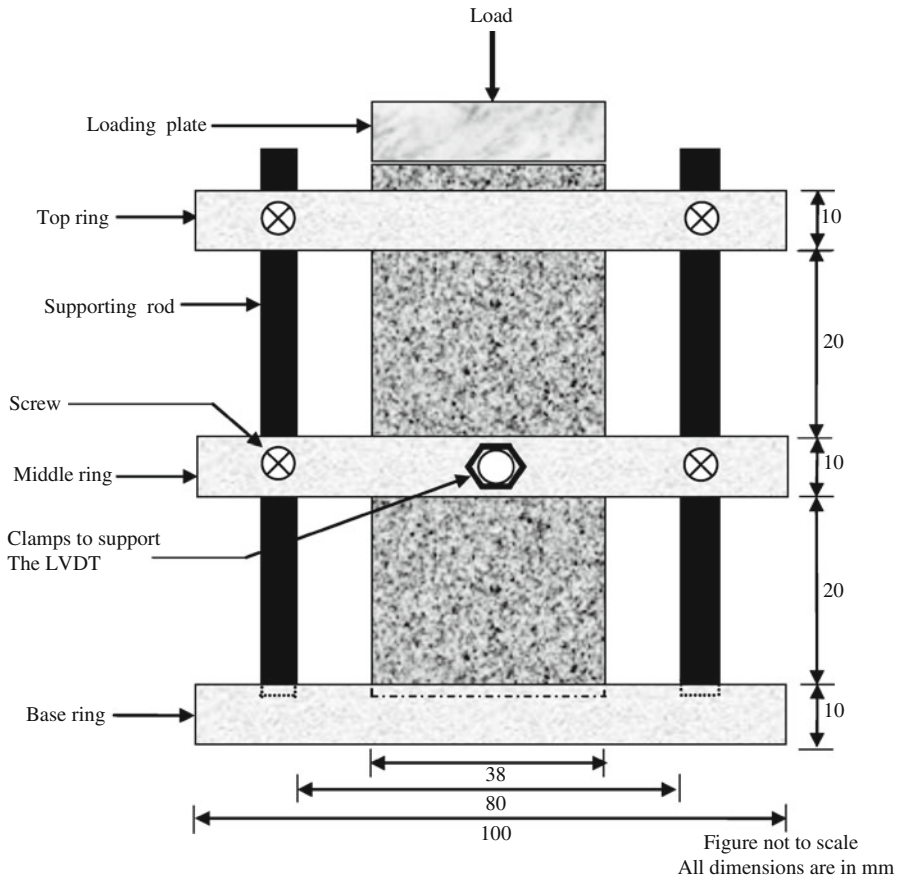

Fig. 1 Details of the sample cage

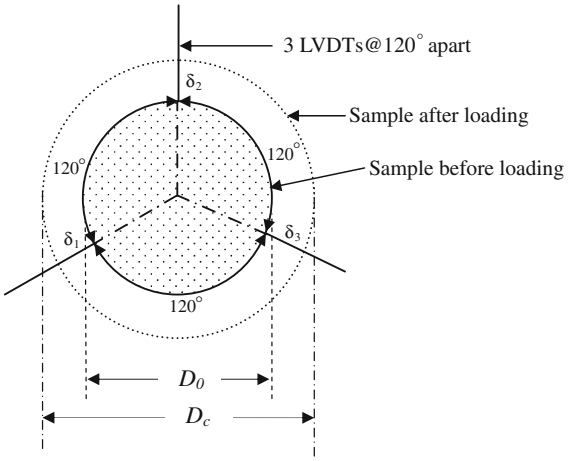

Fig. 2 Details of the positioning of LVDTs

and Greening 2001). Eq. 5 (Dyvik and Madhus 1985; Leong et al. 2005) was then employed for estimating the maximum free lateral deflection, Δh, of the piezoceramic elements for an excitation voltage V (=20V). Δh for these piezoceramic elements was numerically found to be about 1 μm, which induces a shear strain <0.001%.

Table 3 Properties of the piezoceramic elements used

Property	Value
Piezoelectric charge constant [$\times 10^{-12}$ C/N]	−170
Piezoelectric voltage constant [$\times 10^{-3}$ Vm/N]	−11
Relative dielectric constant	1,750
Density [kg/m^3]	7,650
Elastic constant [$\times 10^{-12}$ m^2/N]	16
Dimension (length × width × thickness) in mm	15 × 12 × 0.65

$$\Delta h = 3d \cdot V \cdot \left(\frac{l}{h}\right)^2 \cdot \left(1 + \frac{t_1}{h}\right) \quad (5)$$

where, d is the piezoelectric charge constant, t_1 is the thickness of the central electrode, V is the applied

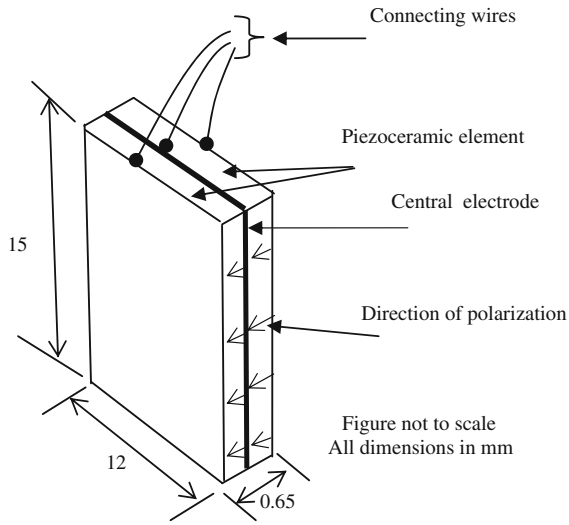

Fig. 3 Details of the piezoceramic elements used in present study

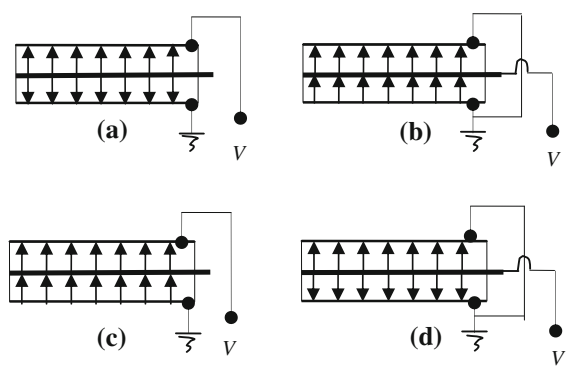

Fig. 4 Different configurations of piezoceramic elements benders (**a** and **b**) and extenders (**c** and **d**)

voltage, h is the thickness and l is the free length of the piezoceramic material.

The transmitter was then excited with a single sine-wave of certain amplitude and frequency, f, which is generated from a function generator developed by Bartake et al. (2008). The receiver is connected to a filter, amplifier circuitry, which is then connected to a digital oscilloscope. The oscilloscope also receives a direct sine-wave from the function generator. Sine-wave recorded by the oscilloscope was then processed to determine the time lag, t, between input and output waves. Later, V_s and V_p were computed by dividing the tip-to-tip distance of the bender elements (transmitter and receiver) with t. For calibration purpose, V_s and V_p were measured on some standard materials. Using Eq. (4), v was computed for rubber, stainless steel, and cork and was found to be 0.5, 0.29 and 0, respectively, which match very well with the results reported in the literature (Tarantino et al. 2005; Venkatramaiah 2006; Gercek 2007).

3 Results and Discussions

Load-deformation charactersitics for the sand samples were obtained corresponding to three trials on identical samples as depicted in Fig. 5a for sample SS1. For these tests the dry density was found to be 1.5 ± 0.1 g/cc. It can be noted from the figure that, beyond certain initial nonlinear deformation, the deformations vary linearly with the applied stress.

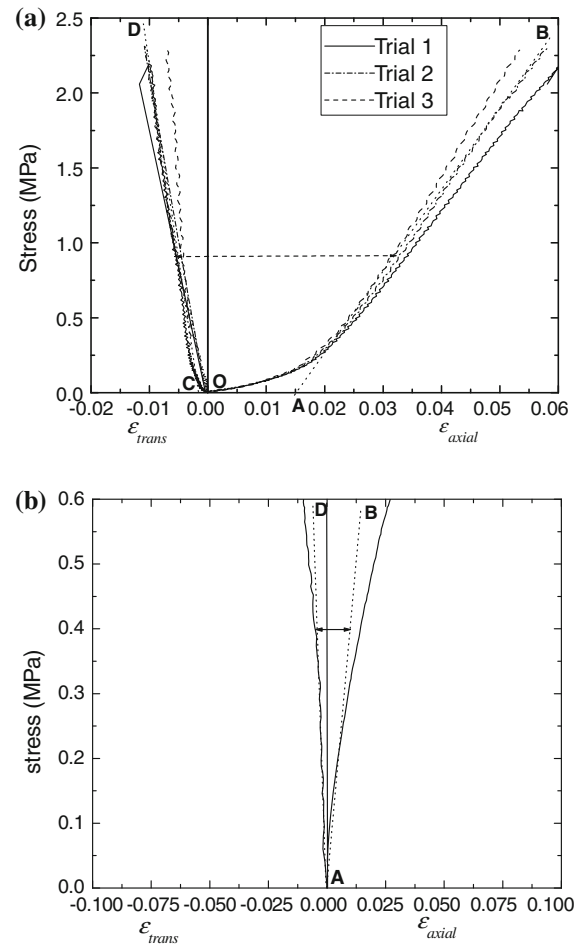

Fig. 5 Typical load-deformation characteristics for (**a**) sample SS1 and (**b**) clayey samples

Table 4 Experimental results for sand samples

Sand	Sample	e	γ_t (kN/m^3)	V_s (m/s)	V_p (m/s)	$E_{expt.}$ (MPa)	v_{expt}
SS1	1	0.76	15.1	86	143	32.6	0.24
	2	0.84	15.1	65	111	12.2	0.23
	3	0.83	15.9	67	109	10.6	0.16
	4	0.84	16.6	59	101	14.0	0.26
	5	0.79	17.8	53	105	8.2	0.30
SS2	6	0.72	15.5	64	109	20.2	0.28
	7	0.82	15.3	44	79	20.3	0.30
	8	0.83	15.9	45	92	25.4	0.37
	9	0.85	16.4	44	79	24.5	0.34
	10	0.79	17.8	42	76	25.7	0.25
SS3	11	0.71	15.5	67	114	30.9	0.25
	12	0.86	14.9	41	74	34.9	0.29
	13	0.85	15.8	47	84	24.9	0.27
	14	0.82	16.7	41	65	29.9	0.16
	15	0.79	17.8	33	55	28.1	0.20

As such, the linear relationships represented by AB and CD were considered for determining v_{expt} (v, obtained from the load-deformation characteristics). Corrections OC and OA were applied to ε_{trans} and ε_{axial}, respectively, for precise value of the v_{expt}. The value of v_{expt}, for different coarse-grained soil samples is listed in Table 4. Figure 5b depicts typical load-deformation curves, for clays. In order to determine v_{expt}, tangents AB and AD were drawn to the axial and transverse responses of the load-deformation characteristics, respectively. The value of v_{expt} for the clay samples are listed in Table 2.

If ε_1, ε_2 and ε_3 are the strains computed by using the deformations recorded by the three lateral LVDTs, then the resultant strain in transverse direction, ε_{trans}, can be obtained as follows (Gere and Timoshenko 1987):

$$\varepsilon_{\text{trans}} = \frac{\varepsilon_1 + \varepsilon_2 + \varepsilon_3}{3} + \frac{\sqrt{2}}{3} \cdot \sqrt[2]{(\varepsilon_1 - \varepsilon_2)^2 + (\varepsilon_2 - \varepsilon_3)^2 + (\varepsilon_3 - \varepsilon_1)^2}. \quad (6)$$

The corresponding stresses are computed as, P/A_c, where P is the axial load applied on the sample and A_c is the corrected area, computed as:

$$Ac = \pi \cdot \frac{(D_c)^2}{4} \quad (7)$$

where, D_c is the corrected diameter, after successive deformation in the sample, computed as follows:

$$D_c = D_o + \frac{2}{3}(\delta_1 + \delta_2 + \delta_3) \quad (8)$$

where, D_o is the initial diameter of the sample and δ_1 δ_2 and δ_3 are the transverse deformations of the soil sample as recorded by the three LVDTs.

The elastic modulus, E_{expt}, of the sample was obtained by determining the slope of the linear portion of the load-deformation (longitudinal strain) characterisitcs. Here, it is worth mentioning that when tested at different strain rates, the linear portions of the load-deformation characterisitcs remain almost same, as depicted in Fig. 6.

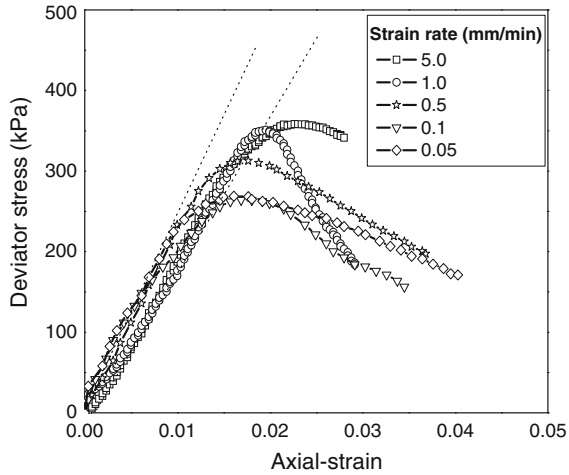

Fig. 6 Deviatric stress versus axial strain characteristics of clays corresponding to different strain rates

For a material in an infinite, linear, elastic, isotropic and homogeneous continuum and for compression mode (plane wave), the following relationship is valid (Santamarina et al. 2001):

$$\frac{\delta^2 u_x}{\delta t^2} = \frac{M}{\rho} \cdot \frac{\delta^2 u_x}{\delta x^2} (P-\text{wave equation}) \tag{9}$$

where, u_x is the particle motion in x-direction and M is the constraint modulus. Similarly, for the shear mode (plane wave) the following relationship is valid:

$$\frac{\delta^2 u_y}{\delta t^2} = \frac{G}{\rho} \cdot \frac{\delta^2 u_y}{\delta x^2} (S-\text{wave equation}) \tag{10}$$

where, u_y is the particle motion in y-direction.

Substituting, $u_x = Ae^{j(\omega t - \kappa\chi)}$ and $u_y = Ae^{j(\omega t - \kappa\chi)}$ in Eqs. (9) and (10), the following can be obtained: $\omega/\kappa = \sqrt{(M/\rho)}$and $\omega/\kappa = \sqrt{(G/\rho)}$ for P- and S-waves, respectively.

where, t is the time, A is the maximum amplitude of the motion, $\omega = 2\pi/T$ is the temporal angular frequency, $\mathrm{k} = 2\pi/\lambda$ is the spatial frequency or wave number, T is the time period and λ is the wave length.

However, $\omega/\kappa = \lambda/T$ which represents the wave velocity. Hence,

$$V_p = \sqrt{(M/\rho)} \tag{11}$$

$$V_s = \sqrt{(G/\rho)} \tag{12}$$

From Eqs. (11) and (12), the following can be derived:

$$(V_p/V_s)^2 = M/G \tag{13}$$

For an isotropic linear-elastic continuum:

$$\mathrm{M} = \frac{E(1-\nu)}{(1+\nu)\cdot(1-2\nu)}. \tag{14}$$

Equation (4) can be obtained by substituting the values of M and G from Eqs. (14) and (2), respectively, into Eq. (13). Further, experimentally obtained Poisson's ratio for different samples, v_{expt}, were compared to those, obtained by using Eq. 4, $v_{\mathrm{Eq.\ 4}}$, as depicted in Fig. 7. It can be observed from the figure that the data fit within 95% prediction limits. Moreover, it can be observed that as expected, v_{expt} is dependent on the water content of the soil mass, w, and it increases almost linearly with w, as depicted in Fig. 8. However, when v_{expt} is plotted against plasticity index, PI, a cloud of data is observed, as depicted in Fig. 9. A poor correaltion between these parameters is due to the fact that, unlike

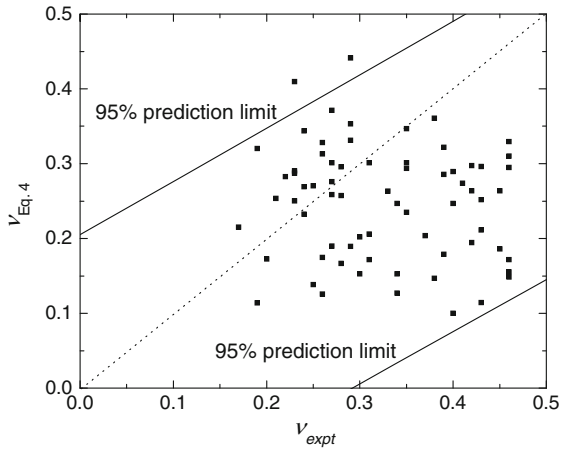

Fig. 7 The comparison of Poisson's ratios obtained from experiments and Eq. 4

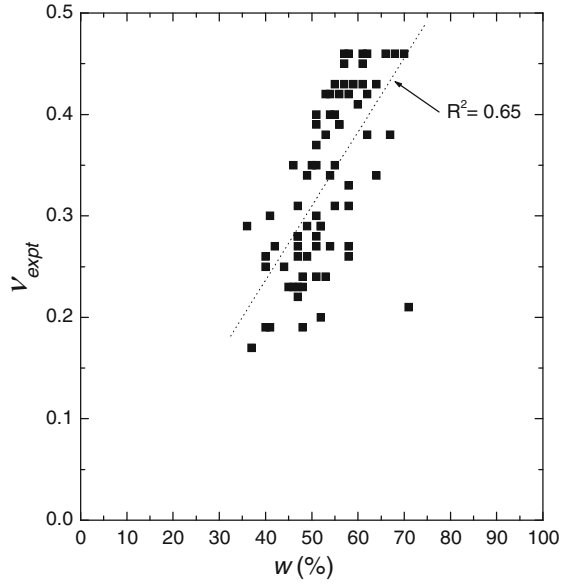

Fig. 8 The variation of Poisson's ratio with water content

w, the PI, being an index property of the soil, will not be able to represent its elastic properties (viz., v).

Further, as depicted in Fig. 10, the elastic modulus of the samples obtained from the triaxial tests, E_{expt}, is compared to that obtained by substituting G and v from Eqs. (3) and (4), respectively, in Eq. 2 (defined as $E_{\mathrm{Eq.\ 2}}$). It can be noted that $E_{\mathrm{Eq.\ 2}}$ is 7.5 times higher than the E_{expt}. This is consistent with the fact that the piezoceramic elements yield low-strains (<0.001%) in

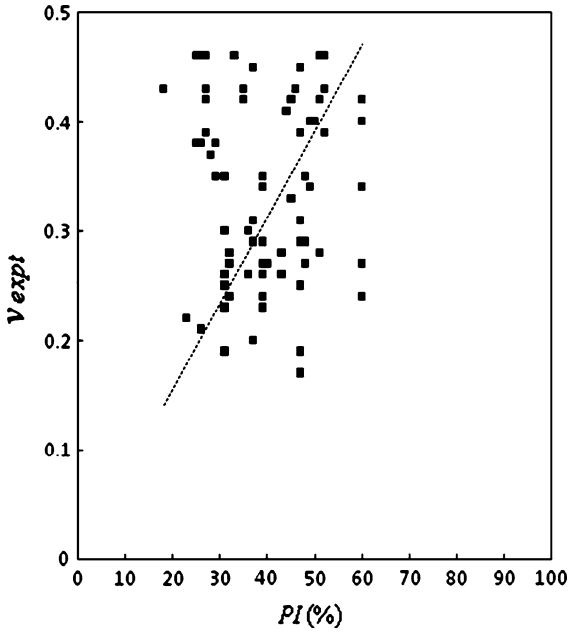

Fig. 9 The variation of Poisson's ratio with plasticity index

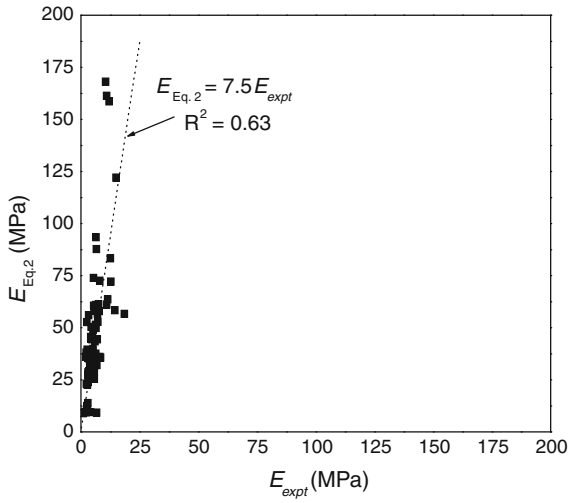

Fig. 10 Comparison between the estimated and experimental values of elastic modulus

the soil mass (Dyvik and Madhus 1985; Leong et al. 2005) and hence higher elastic modulus.

4 Conclusions

Investigations has been conducted on soils of different types (clays and sands) in their disturbed and undisturbed forms by resorting to piezoceramic tests and conventional triaxial tests (i.e., strain controlled uniaxial compression tests). Details of the methodology are presented in this paper and it has been demonstrated that application of piezoceramic elements yields the Poisson's ratio and the elastic modulus of the soils quite easily, particularly for the soft clays and sands. Poisson's ratio obtained from the triaxial testing was found to be dependent on the water content of the soil mass, *w*, and it increases almost linearly with *w*. The elastic modulus, obtained from the wave velocities was found to be 7.5 times more than that obtained from the triaxial testing.

References

Agarwal TK, Ishibashi I (1991) Multi-directional wave velocity by Piezoelectric crystals. In: Bhatia and Blaney (Eds) Proceedings, recent advances in ınstrumentation, data acquisition and testing in soil dynamics, Orlando, FL, pp 102–117

Ayres A, Theilen F (2001) Relationship between P- and S-wave velocities and geological properties of near-surface sediments of the continental slope of the Barents Sea. Geophys Prospect 47(4):431–441

Bartake PP, Patel A, Singh DN (2008) Instrumentation for bender element testing of soils. Int J Geotech Eng 2(4): 395–405

Bragg RA, Andersland OB (1982) Strain dependence of Poisson's ratio for frozen sand. In: Proceeding of 4th Canadian permafrost conference, pp 365–373

Brocanelli D, Rinaldi V (1998) Measurement of low-strain material damping and wave velocity with bender elements in the frequency domain. Can Geotech J 35:1032–1041

Dyvik R, Madhus C (1985) Lab measurement of G_{max} using bender elements. In: Proceeding of the ASCE annual convention: advances in the art of testing soils under cyclic conditions, p 7

Gercek H (2007) Poisson's ratio values for rocks. Int J Rock Mech Min Sci 44(1):1–13

Gere JM, Timoshenko SP (1987) Mechanics of materials, Van Nost. Reinhold, US, ISBN-13

Huang YT, Huang AB, Kuo YC, Tsai MD (2004) A laboratory study on the undrained strength of a silty sand from central western Taiwan. Soil Dyn Earthq Eng 24:733–743

Jain S (1988) S-wave velocity and Poisson's ratio from shear waves observed in P-wave data in an offshore basin. Can J Explor Geophys 24(1):32–47

Jovicic V, Coop MR, Simic M (1996) Objective criteria for determining G_{max} from bender element tests. Geotechnique 46(2):357–362

Kim DS, Stokoe KH (1992) Characterization of resilient modulus of compacted subgrade soils using resonant column and torsional shear tests. Trans Res Rec 1369:89–91

Landon MM, DeGroot DJ, Sheahan TC (2007) Nondestructive sample quality assessment of soft clay using shear wave velocity. J Geotech Geoenv Eng 133(4):424–432

Lees JM, Wu H (2000) Poisson's ratio and porosity at Coso Geothermal area, California. J Volcan Geotherm Res 95:157–173

Leong EC, Yeo SH, Rahardjo H (2005) Measuring shear wave velocity using bender elements. Geotech Test J 28(5):1–11

Lings ML, Greening PD (2001) A novel bender/extender element for soil testing. Geotechnique 51(8):713–717

Lohani TN, Imai G, Shibuya S (1999) Determination of shear wave velocity in bender element test. In: Proceedings of second international conference on earthquake geotechnical engineering, vol 1. Lisbon, Portugal, pp 101–106

Luna R, Jadi H (2000) Determination of dynamic soil properties using geophysical methods. In: Proceedings of the first ınternational conference on the application of geophysical and NDT methodologies to transportation facilities and ınfrastructure, St. Louis, MO

Mancuso C, Vassallo R, d'Onofrio A (2002) Small strain behavior of a silty sand in controlled-suction resonant column-torsional shear tests. Can Geotech J 39(1):22–31

Phani KK (2008) Correlation between ultrasonic shear wave velocity and Poisson's ratio for isotropic porous materials. J Mater Sci 43:316–323

Samsuri A, Herianto H (2004) Comparison of sandstone mechanic properties using acoustic test and direct uniaxial test. 18th symposium of Malaysia chemical engineers, pp 13–14

Santamarina JC, Klein KA, Fam MA (2001) Soil and Waves. John Wiley and Sons Ltd., NY

Sawangsuriya A, Fall M, Fratta D (2008) Wave-based techniques for evaluating elastic modulus and Poisson's ratio of laboratory compacted lateritic soils. Geotech Geol Eng 26:567–578

Tarantino A, Romero EJ, Cui YJ (2005) Advanced experimental unsaturated soil mechanics. In: Proceedings of the ınternational symposium on advanced experimental unsaturated soil mechanics, Trento, Italy, pp 27–29

Venkatramaiah C (2006) Geotechnical engineering, 3rd Edn, New Age International, EAN: 788122417937

Zeng X, Tammineni V (2006) Measurement of small-strain modulus of gravelly soils using oedometer equipped with piezoelectric sensors. Pavement mechanics and performance, geotechnical special publication. ASCE 154:239–246